

# Optimizing Techno-Economic Resilience in Microgrids: A Multi-Objective Strategy for Post-Attack Recovery

Mehdi Ahmadi Jirdehi<sup>1\*</sup>, Hazhir Dousti<sup>2</sup>

<sup>1</sup> Department of Electrical Engineering, Faculty of Electrical Engineering, Kermanshah University of Technology, Kermanshah, Iran

m.ahmadi@kut.ac.ir

<sup>2</sup> Department of Electrical Engineering, Faculty of Electrical Engineering, Kermanshah University of Technology, Kermanshah, Iran

h.dousti73@gmail.com

---

**Keywords:**

attacks,  
distributed generation  
resources,  
dynamic reconfiguration,  
microgrid,  
techno-economic response.

**Abstract:** Given the increasing expansion of power grids and their vulnerability to malicious attacks and natural disasters, it is necessary to consider measures to enhance the resilience of these networks against such events. Otherwise, irreparable damages may occur. This article investigates enhancing the resilience of a 33-bus IEEE power network against cyberattacks. It proposes a dynamic reconfiguration method that strategically switches to prevent network collapse and to reduce operational costs while maintaining voltage stability. Using MATLAB simulations, the study demonstrates that this approach effectively improves the network performance and the resilience in the face of cyber threats. The integration of renewable resources and a multi-objective optimization algorithm further support the management of distributed generation resources. Overall, the findings highlight the importance of adaptive strategies in maintaining the stability and efficiency of power microgrids under attack.

---

**Original Research Article**

**Paper History:**

Received: 17/08/2024

Revised: 27/09/2024

Accepted: 28/09/2024

Available online: 28/09/2024

---

**How to cite this article:** Ahmadi Jirdehi, M., Dousti, H., "Optimizing Techno-Economic Resilience in Microgrids: A Multi-Objective Strategy for Post-Attack Recovery", Energy Engineering and Management, Vol. 13, No. 4, PP. 14-25, 2024. <https://doi.org/10.22052/eem.2024.255316.1082>

© 2023 University of Kashan Press.

This is an open access article under the CC BY license. (<http://creativecommons.org/licenses/by/4.0/>)



## 1. Introduction

Optimal generation management within microgrids has advanced significantly in recent years. Many of the current studies, however, do not have a thorough management strategy that makes use of the network's control capabilities to their fullest. For instance, volt-var control has frequently been used in earlier works [1, 2] to regulate the distribution network. The majority of studies on the best way to operate a microgrid with demand response has been on finding ways to reduce operating expenses by strategically distributing small amounts of energy. These studies frequently provide a standalone solution to the issue for a particular microgrid without taking the distribution network or other micro-networks into account.

In reference [3], an optimization-based solution is proposed for the optimal distribution of Distributed Generators (DGs) and Distributed Storage (DS) units in isolated microgrids. This method takes into account the microgrid's overall operating costs as well as the environmental damage that program DGs cause. The National Evolutionary Algorithm (NEA) is employed to solve the optimization problem. Additionally, reference [3] introduces a two-level control scheme for DGs, which includes:

1. Low-level control (decentralized control): At this level, each DG independently controls the voltage and frequency of a specific section of the network.
2. High-level control (centralized control): This level involves coordination control by a Central Controller (CC) to optimize the target functions across DGs.

Overall, the existing literature has made progress in optimizing generation management within microgrids, but there is a noticeable lack of comprehensive management plans that consider the entire network and leverage the control potential available.

Reference [3] presents an intelligent energy management system (SEMS) designed to minimize a microgrid's operating expenses. SEMS consists of three phases: forecasting the generation power of non-programmable sources (such as photovoltaic (PV)), storage management, and an optimization stage. The emphasis in [3] is placed on storage devices and their optimal utilization under varying energy prices. The objective function used in [3] incorporates control variables such as the economic distribution of load, the utilization of microresources, and the intelligent management of storage devices. The proposed method employs a multi-objective optimization algorithm to effectively manage the microgrid, considering factors such as operational cost, pollution caused by microresources, and the upstream network.

An algorithm that generates a set of non-dominant points [4] solves the microgrid management challenge. Then, the network operator, taking into account the needs of the network, chooses an appropriate solution from this group. The power output of programmable distributed generation and storage generators is the control variable used in these references. Nevertheless, the main focus of

these publications is on the microgrid's economic distribution of microresources; storage management, demand response, and other control mechanisms are only briefly mentioned.

It is important to note that the integrated management of a microgrid should consider various objective functions such as operating costs, losses, pollution caused by microresources and the upstream network, and voltage deviation. Most of the aforementioned references prioritize the minimization of the microgrid's operating costs as the main objective function. Only a few references such as [3] investigate the impact of microresources and the upstream network on pollution as an additional objective function.

Furthermore, the discussion on microgrid management in these references primarily revolves around the economic distribution of microresources while neglecting other objective functions. Some references separately address managing active distribution networks using methods like voltage-variable control and reconfiguration [7–10]. With the goal to transform traditional distribution networks into smart networks, reference [10] provides an approach for optimal load flow in unbalanced distribution networks that focuses on using the switching potential in capacitors and tap transformers. However, microgrid management is not extensively discussed in this reference.

On a different note, integrated energy systems include combined heat and power (CHP) systems, which have drawn interest from international publications [11]. Recent advancements in CHP systems include improved technical capabilities and the alleviation of challenges in creating experimental setups through suitable policies [12]. The economic operation of CHP systems, particularly those based on fuel cells, has been studied in [12], where four modes of heat dispatching recovery are compared. An examination of a gas turbine and battery-powered CCHP (combined cooling, heating, and power) system demonstrates the benefits of CCHP, including storage devices [13]. However, the operating cost of this system is not explicitly considered.

Integrated energy systems-- involving various sources of energy like fuel cells, wind turbines (WT), PVs, micro turbines, diesel generators, and battery storage systems-- have been investigated [14]. The operation cost of these systems is optimized with a focus on reducing emissions of  $\text{NO}_x$ ,  $\text{SO}_2$ , and  $\text{CO}_2$ . A study on an energy system comprising wind energy, PV, heat recovery boilers, and batteries has been conducted [15]. The analysis calculates the system's operation cost and explores the impact of battery use and electricity tariffs on energy transportation costs. Nevertheless, optimal planning of different energy sources and determining the minimum cost of daily operation in the integrated energy system are not explicitly addressed.

One specific study [16] examines the economic viability of a combined WT and proton membrane fuel cell (PEMFC) CHP system using an evolutionary algorithm. This research presents four different methods

to address heat recovery. Another study proposes an optimization model for a CHP system incorporating multiple distributed energy sources [17]. The objective of the model is to reduce the operating costs of the system.

The cost-effectiveness of a CHP system with a storage system installed in a home is examined in the context of home energy systems [18]. The integrated energy system includes a fuel cell, a battery, thermal loads, and electrical loads. The study models the economic aspects of the system and employs the Colonial Competition Algorithm (CCA) to minimize operating costs. Factors such as battery efficiency and electricity tariffs are considered, highlighting the significant impact of battery efficiency on system costs.

Several papers focus on the modeling and optimizing integrated energy systems, aiming to minimize operating costs. For instance, one paper models an integrated energy system and employs the Coordinated Search Algorithm (HSA) to minimize operating costs [19]. However, battery charging and discharging efficiency is not considered in this particular study. Another paper explores the economic model of an integrated energy system in greater detail and utilizes CCA to minimize the global cost function [19]. A comparison between the optimization results obtained using HSA and CCA demonstrates the superior performance of the proposed approach.

The subsequent sections of the article outline the smart home energy system, energy management strategies, problem formulation, limitations, optimization techniques such as CCA, and simulation results.

The electrical industry has changed its focus to small-scale power plants connected to the grid, mostly based on renewable energy sources, in response to growing industrial demands as well as the economic and environmental difficulties associated with large-scale power plants [20, 21]. Electricity generated at the point of consumption is referred to as distributed generation (DG) and is usually produced by the relatively small generators that are directly connected to the distribution network [22]. Because of their ability to lower transmission and distribution costs, these resources can save money. Furthermore, distributed generation makes it possible to integrate renewable energy sources into the process of producing power.

The resilience of cyber-physical power systems (CPPSs) to cooperative attacks is examined in [23]. It develops a cooperative optimization to increase resilience, constructs islanded systems with repaired components, and suggests the detection methods for both physical and cyberattacks.

The innovations of the article include:

1. **Dynamic Reconfiguration Method:** The study introduces a novel dynamic reconfiguration strategy that enables the microgrid to adaptively change its configuration in response to cyber threats. This method focuses on strategic switching to maintain stability and efficiency during and after an attack.

2. **Multi-Objective Optimization Framework:** The paper employs a multi-objective optimization algorithm

that simultaneously addresses operational cost reduction, voltage stability, and resilience against cyber threats. This comprehensive approach enhances the decision-making for managing distributed generation resources.

3. **Integration of Renewable Resources:** The research emphasizes the integration of various renewable energy sources (solar, wind, etc.) into the microgrid management strategy. It models the cost functions of these resources, contributing to a more sustainable and economically viable energy system.

4. **Simulation-Based Validation:** The effectiveness of the proposed methods is validated through extensive MATLAB simulations, demonstrating significant improvements in network performance, including the prevention of collapse and the reduction of excessive operational costs during cyber-attack scenarios.

5. **A focus on Post-Attack Recovery:** Unlike many existing studies that focus on attack detection or prevention, this paper emphasizes the recovery strategies after the occurrence of an attack, making it a valuable contribution to the field of power grid resilience.

The effectiveness of the suggested strategy in strengthening the system's resistance to hybrid attacks is shown by the simulation results. Cyber-physical attacks that target both the physical and the cyber layers of the electrical grid were observed at [24]. The proposed attack strategy involves disconnecting a transmission line and misleading the management center with a fictitious systemic outage, aiming to interfere with topology information and to increase the risk of cascade failure. Simulation results confirm the effectiveness of the attack strategy. Using the highly random trees algorithm and kernel principal component analysis for dimensionality reduction. Reference [25] suggests a novel method for detecting cyberattacks in smart grid networks.

## 2. Optimal Energy Management in a Hierarchical Plan

In this section, a novel approach to execute optimal energy management is proposed, where the best configuration to lower operating costs and to enhance technical indicators is taken into account, and a multi-objective particle cumulative optimization algorithm is used to optimize the objective function. As a result, the cost functions of distributed solar, wind, and other resources will be modeled first in the sections that follow. After that, the system's objective function will be addressed utilizing the particle algorithm to optimize the multi-objective function while taking into account the demand and the response schedule and the uncertainty of the consumption court.

This article discusses the issue of a microgrid's coordinated and ideal energy management in relation to dispersed generations when a critical bus fails as a result of a cyberattack. This solution's primary objectives are to lower operating costs and boost microgrid dependability following an attack.

According to the suggested method, shown in Figure 1, a new strategy for implementing coordinated energy management to lower the costs associated with power

generation resources and consumption management is being implemented. This strategy involves implementing the demand response program as an optimization program concurrently. It is suggested that the objective function be optimized using an optimization algorithm such as particle aggregation, keeping in mind the previously indicated objectives (lowering costs and raising reliability). In this regard, initially, the cost-operate modeling of DGs, like wind and solar power systems, will be covered. After that, the objective function of the system will be introduced by considering the reliability indicators, and the objective function will be optimized. It is solved using the desired algorithm.

### 2.1. Modeling the cost function of distributed solar and wind generation resources

The output power of renewable energy sources is determined by the availability of primary energy sources, such as wind speed and solar radiation intensity. Depending on the location of the installation, the weather, and the time of day, photovoltaic power plant generation is directly correlated with the amount of solar radiation on Earth's surface.

The temperature ( $T_{amp}$ ) of the cells and the power of the sun's radiation ( $G_{T(t)}$ ) both affect the output power of photovoltaic arrays, the following equation of which is (1) [20]:

$$P_{PV}(t) = \left[ P_{PV,STC} \times \frac{G_{T(t)}}{1000} \times [1 - \gamma(T_j - 25)] \right] \times N_{PVS} \times N_{PVP} \quad (1)$$

$$T_j = T_{amp} + \frac{G_{T}}{G_{T,STC}} \times (NOCT - 20) \quad (2)$$

$P_{PV(t)}$  represents power output of the photovoltaic (PV) system at time t (in watts).  $P_{(PV,STC)}$  indicates rated power of the PV system under Standard Test Conditions (STC) (in watts).  $G_{T(t)}$  represents solar irradiance at time t (in watts per square meter).  $\gamma$  denotes power temperature coefficient (typically expressed as a percentage change in power per degree Celsius).  $T_j$  is temperature of the photovoltaic cells (in degrees Celsius).  $T_{amp}$ : represents ambient temperature (in degrees Celsius) at the time of measurement.  $N_{PVS}$  represents the number of photovoltaic panels in the system.  $N_{PVP}$  indicates the number of strings of photovoltaic panels in the system. NOCT represents Nominal Operating Cell Temperature, which indicates the temperature of the PV cells under specific conditions (usually around 45°C to 50°C in typical conditions).

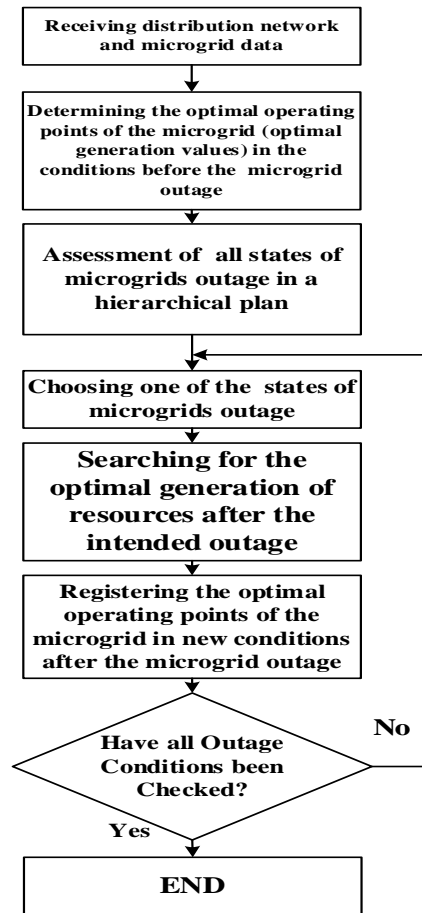


Fig. 1: The steps of the proposed method for power management in a microgrid when the microgrid outage

The output power of the generator at the point of maximum power, the rated power of PV at the point of maximum power and standard conditions, the amount of radiation in standard conditions, the temperature coefficient of power at the point of maximum power, the temperature of solar cells, the nominal operating temperature of the cell, and the number of series and parallel modules are all included in equations (1) and (2) for  $P_{PV,t}$ ,  $P_{PV, STC}$ ,  $G_{T,t}$ ,  $T_j$ ,  $N_{PVS}$ ,  $N_{PVP}$ , and NOCT, respectively. Wind speed determines how much power a wind turbine can produce. Variations in wind speed can be fleeting, hourly, daily, or partial. Equation (3) is therefore used [20, 27] to model the active power produced by the wind turbine:

$$P_{wt}(v) = \begin{cases} 0 & \text{if } v < V_{ci} \\ P_R(A + Bv + Cv^2) & \text{if } V_{ci} < v < V_r \\ P_R & \text{if } V_r < v < V_{co} \\ 0 & \text{if } V_{co} < v \end{cases} \quad (3)$$

In equation (3)  $V_{ci}$ ,  $V_{co}$ ,  $V_r$  are respectively the lower and upper cutoff, the wind turbine's nominal speed, the nominal power, and A, B, and C The coefficients are related to the turbine. Due to the unavailability of data related to solar radiation and wind speed in a specific area at the time of simulation, a combination of information from two different areas is used for this purpose. It is better to use comprehensive information for an area to make this assessment more accurate.

## 2.2. Microturbine Cost Modeling

The microturbine's operating costs, which comprise both operating and emission costs, are modeled by equation (4) [20]. The literature review of the recent works in the related field and the subject of the paper must be first presented. Then, the justification of using the new contribution must be explained and in the end, the main contribution of the work should briefly be explained.

$$C_{MT,t} = C_{MT,t}^{OP} + C_{MT,t}^{EM} \quad (4)$$

$C_{MT,t}$  represents the total cost associated with the microturbine (MT) at a specific time  $t$ . It encompasses all operational and emergency-related expenses.  $C_{MT,t}^{OP}$  denotes the operating costs of the microturbine at time  $t$ . These costs typically include expenses related to fuel, maintenance, labor, and other operational factors necessary for the normal functioning of the microturbine.

$C_{MT,t}^{EM}$  represents the emergency costs at time  $t$ . These costs might arise from unexpected events such as system failures, environmental compliance issues, or the additional measures taken to mitigate risks during emergencies.

## 2.3. Diesel Generator Cost Modeling

Equations (5), (6), (7), and (8) represent the cost of operating a diesel generator, which includes fuel and emission costs [20].

$$C_{DG,t} = C_{DG,t}^{OPR} + C_{DG,t}^{EMI} \quad (5)$$

$$C_{DG,t}^{OPR} = C_{Fuel,DG} \quad (6)$$

$$C_{Fuel,DG} = \begin{cases} a_{DG}P_{DG}^2 + b_{DG}P_{DG} + c_{DG} & \text{if } 0 < P_{DG} < P_{DG}^{rated} \\ 0 & \text{if } P_{DG} = 0 \end{cases} \quad (7)$$

$$C_{DG,t}^{EMI} = (C_{CO_2} \times CO_2 + C_{SO_2} \times SO_2 + C_{NO_x} \times NO_{x,DG}) \times P_{DG} \quad (8)$$

In equation 5,  $C_{DG,t}$  represents the total cost of operating the diesel generator (DG) at a specific time ( $t$ ). It includes both operational and emission-related costs.  $C_{DG,t}^{OPR}$  represents the operational cost of the diesel generator at time ( $t$ ).  $C_{DG,t}^{EMI}$  indicates the emission costs associated with operating the diesel generator at time ( $t$ ). In equation 6,  $C_{DG,t}^{OPR}$  represents, as defined earlier, the operational cost of the diesel generator. It is expressed in terms of fuel costs.  $C_{Fuel,DG}$  represents the cost associated with the fuel used by the diesel generator. In equation 7,  $a_{DG}$ ,  $b_{DG}$ ,  $c_{DG}$  are coefficients that define the cost function for fuel. They may represent fixed, linear, and quadratic components of fuel costs, respectively.  $P_{DG}$  is the power output of the diesel generator.  $P_{DG}^{rated}$  represents the rated power output of the diesel generator. The piecewise function indicates that:

- If  $0 < P_{DG} < P_{DG}^{rated}$ , fuel costs are calculated using the quadratic equation.

- If  $P_{DG} = 0$ , the fuel cost is zero.

In equation (8), the parameters include the following:

- Penalty for CO<sub>2</sub> generation by microturbine
- Generation penalty by microturbine

- No generation penalty by microturbine
- Fine for producing CO<sub>2</sub> by diesel generator
- Fine for producing SO<sub>2</sub> by diesel generator
- N<sub>ox</sub> generation penalty by diesel generator

## 2.4. Cost of Energy Storage System

With the increasing integration of electric vehicles and renewable energy sources in current hybrid systems, maintaining the frequency within the permitted range has become more challenging. By assisting in keeping supply and demand in balance, the extra energy units help to prevent frequency variation in real time. An energy storage system (ESS) can be used as auxiliary energy storage to compensate for frequency deviations in sudden changes in generation from renewable sources. Operating limits for energy storage are defined by several factors such as battery unit layout, backup duration, temperature, battery unit lifetime, discharge depth, energy storage sources, renewable generation in the grid, etc. A storage unit can be specified as follows [20]:

$$P_{ESS}(t) = \begin{cases} P_{ch}(t) & \text{if } \begin{cases} P_{PV}(t) + P_{WT}(t) + P_{DG}(t) \\ + P_{FC}(t) + P_{MT}(t) \\ + P_g(t) - P_D(t) \end{cases} \geq 0 \end{cases} \quad (9)$$

$$P_{ESS}(t) = \begin{cases} P_{dis}(t) & \text{if } \begin{cases} P_{PV}(t) + P_{WT}(t) + P_{DG}(t) \\ + P_{FC}(t) + P_{MT}(t) \\ + P_g(t) - P_D(t) \end{cases} < 0 \end{cases} \quad (10)$$

Only one operating condition at a time-- i.e., charging or discharging-- is conceivable for a storage unit. The storage capacity related to each condition is calculated as follows:

Charging mode:

$$E_{ch}(t) = \left( \frac{P_{DG}(t) + P_{WT}(t) + P_{FC}(t) + P_{MT}(t) - P_D(t)}{\eta_{conv}} + P_{PV}(t) \right) \times \Delta t \times \eta_{ch} \quad (11)$$

$$SOC(t) = SOC(t-1)(1-\sigma) + E_{ch}(t) \quad (12)$$

Discharge mode:

$$E_{dis}(t) = \left( \frac{-P_{DG}(t) - P_{WT}(t) - P_{FC}(t) - P_{MT}(t) + P_D(t)}{\eta_{conv}} - P_{PV}(t) \right) \times \Delta t \times \eta_{ch} \quad (13)$$

$$SOC(t) = SOC(t-1)(1-\sigma) - E_{dis}(t) \quad (14)$$

In equation 11,  $P_{DG}(t)$  stands for power output from the diesel generator at time  $t$ ;  $P_{WT}(t)$  stands for power output from wind turbines at time  $t$ ;  $P_{FC}(t)$  stands for power output from fuel cells at time  $t$ ;  $P_{MT}(t)$  stands for power output from micro turbines at time  $t$ ;  $P_D(t)$  stands for power demand at time  $t$ ;  $\eta_{conv}$  represents efficiency of the conversion process (e.g., from electrical to stored energy);  $P_{PV}(t)$  stands for power output from photovoltaic (solar) panels at time  $t$ ;  $\Delta t$  represent time interval over which the energy is calculated; and  $\eta_{ch}$  depicts the efficiency of the charging process. In equation 12,  $SOC(t)$  stands for a state of Charge of the storage unit at time  $t$ ,  $SOC(t-1)$  for a state of Charge of the storage unit at the previous time step; and  $\sigma$  for a self-discharge rate of the storage unit. In equation 13, similar



terms are used as in equation (11), but here it represents power sources being used to meet demand rather than contributing to charging. The negative signs indicate that these sources are being utilized to discharge energy. Equation 14 is similar to equation (12), but it updates the state of charge based on discharging; the energy discharged is subtracted from the previous state of charge, which also accounts for self-discharge.

On the other hand, useful life power and floating useful life are the two primary parameters that affect a battery's lifetime. The microgrid operator is in charge of figuring out the battery life limiter based on throughput, time, or both. The grid operator must replace the storage bank when a unit's characteristics show that the operational throughput determines the storage lifetime limit since the storage bank's total capacity matches its lifetime operational throughput. The lifetime of a storage unit can be obtained with the following equations:

$$R_{batt} = \begin{cases} \frac{N_{batt} Q_{lifetime}}{Q_{thrpt}} & \text{if limited by throughput} \\ R_{batt, f} & \text{if limited by time} \\ \min \left[ \frac{N_{batt} Q_{lifetime}}{Q_{thrpt}}, R_{batt, f} \right] & \text{if limited by throughput and time} \end{cases} \quad (15)$$

$$C_{bw} = \frac{C_{rep, batt}}{N_{batt} Q_{lifetime} \sqrt{\eta r t}} \quad (16)$$

## 2.5. Network Loss Modeling

The goal of power transmission line designers is always to minimize losses in the grid since they are inevitable phenomena that restrict the transmission power in the lines and always add to the network's expenses. In this project, the load distribution method yields the network's total loss, which is then utilized as one of the factors in the objective function, which is, then, determined using the equation (17) [21, 26].

$$Active\ Losses = \left( \frac{|V|^2}{R_{Z_i}} \right)_{end} - \left( \frac{|V|^2}{R_{Z_j}} \right)_{start} \quad (17)$$

## 2.6. Voltage Deviation Modelling

Reducing the voltage deviation in the distribution network during ideal energy distribution and management is another objective of this study. The amount of voltage deviation is obtained according to equation (18) [21].

$$VD = \sqrt{\sum_{i=1}^{Nb} \left( \frac{V_{S\ standard}}{V_{Base}} - \frac{V_i}{V_{Base}} \right)^2} \quad (18)$$

## 2.7. Micro-Grids Outage Modeling

In this article, according to Figure (2), a typical microgrid of electric loads and distributed generations is formed, which is connected to an upstream distribution network. In these microgrids of loads and energy sources, collisions are minimized. They are located close to each other. According to the figure, the micro-network in buses 17 and 32 is connected to the main distribution

network by the switches in buses 17 to 35 and 32 to 38, which are disconnected and connected according to the operating conditions. Therefore, microgrids are usually operated in two modes: 1) connected to the main grid, and 2) separated from the main grid (island). In a state connected to the grid, energy exchange takes place between the microgrid and the main grid. In this paper, the switchings to connecting microgrids to the main distribution network are modeled with two values of zero for the open state and of one for the connected state in the form of equation (19):

$$CB_i = \begin{cases} 1 & \text{if MG is connected} \\ 0 & \text{if MG is not connected} \end{cases} \quad (19)$$

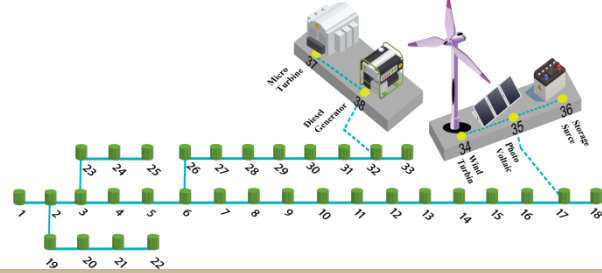


Fig. 2: Schematic of distribution network including microgrids

## 2.8. Problem Formulation

The goal function of this problem includes minimizing and reducing the costs of distributed generation and electricity consumption, as well as reducing the costs of pollution, network losses, and voltage deviation by considering different states of disconnection or connection of microgrids to the main distribution network. Therefore, the objective function is defined as equation (20):

$$Total\ Cost = \left\{ \begin{array}{l} \frac{C_{PV} \times P_{PV}}{PV\ Cost} + \frac{C_{wt} \times P_{wt}}{wind\ turbine\ cost} + \\ \frac{C_{MT,t}}{microturbine\ cost} + \frac{C_{Dg,t}}{Deidel\ cost} + C_{Battery} \end{array} \right\} + \{ \{ (P_{s,t} \times MP_t) \} + CB_i \} \quad (20)$$

## 3. Simulation Results and Discussion

In this section, we will examine and simulate the proposed method for optimal energy management, taking into account the optimal configuration of multiple microgrids in the standard IEEE 33-bus network as illustrated in Figure (3). The study focuses on three microgrids located at buses 17, 22, and 33 within the distribution network as depicted in Figure (2). The electricity generation is achieved through a combination of WTs, PVs, microturbines, and diesel generators while batteries are utilized for energy storage. The evaluation primarily revolves around the optimal distribution of power among the distributed generation sources, considering various scenarios involving the entry and exit of microgrids within a hierarchical control plan. Specifically, we analyze the impact of a physically cyber-attack that removes the line between bus 6 and 7.

The particle algorithm is utilized to optimize the energy generation management system. With an aim to lower the cost of power delivery to the grid, this algorithm calculates the ideal quantity of electricity generation at each time step inside the hybrid system.

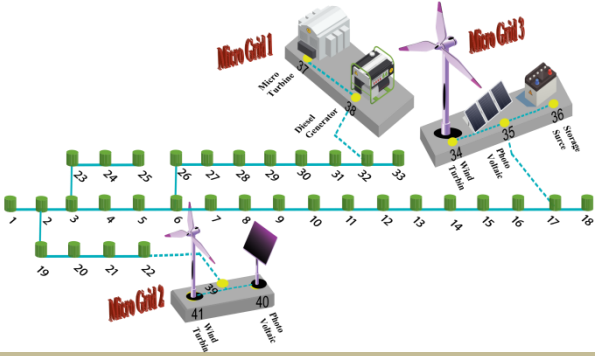


**Fig. 3: Schematic of the modified 33-bus network with connected microgrids**

As the aforementioned figure illustrates, in the studied distribution network, three micro-grids No. (1), (2), and (3) are embedded in buses 17, 22, and 32, respectively, which have solar, wind, and storage sources. They are placed in Bus No. 17, also sources of microturbine, and diesel generator are placed in Bus No. 32, and a wind and photovoltaic system is also placed in Bus No. 22. In the following, information on the location of loads and network lines of 33 buses is displayed in tables (2) and (3), respectively.

**Table 1: Load data for IEEE33 Bus Network**

Node number	Fixed load
	$P(\%$ of total Load)
1	0
2	2.69
3	2.42
4	3.23
5	1.61
6	1.61
7	5.38
8	5.38
9	1.61
10	1.61
11	1.21
12	1.61
13	1.61
14	3.23
15	1.61
16	1.61
17	1.61
18	2.42
19	2.42
20	2.42
21	2.42
22	2.42
23	2.42
24	11.3
25	11.3
26	1.61
27	1.61
28	1.61
29	3.23
30	5.38
31	4.03
32	5.65
33	1.61

**Table 2: Line data for IEEE33 Bus Network**

From_node	To_node	$r/\Omega$	$x/\Omega$
1	2	0.0922	0.047
2	3	0.493	0.2511
3	4	0.366	0.1864
4	5	0.3811	0.1941
5	6	0.819	0.707
6	7	0.1872	0.6188
7	8	0.7114	0.2351
8	9	1.03	0.74
9	10	1.044	0.74
10	11	0.1966	0.065
11	12	0.3744	0.1238
12	13	1.468	1.155
13	14	0.5416	0.7129
14	15	0.591	0.526
15	16	0.7463	0.545
16	17	1.289	1.721
17	18	0.732	0.574
2	19	0.164	0.1565
19	20	1.5042	1.3554
20	21	0.4095	0.4784
21	22	0.7089	0.9373
3	23	0.4512	0.3083
23	24	0.898	0.7091
24	25	0.896	0.7011
6	26	0.203	0.1034
26	27	0.2842	0.1447
27	28	1.059	0.9337
28	29	0.8042	0.7006
29	30	0.5075	0.2585
30	31	0.9744	0.963
31	32	0.3105	0.3619
32	33	0.341	0.5302

### 3.1. Case Study Input Data

Equation (21) of the parts and parameters of the models, given in the third part, introduces the combined power system in the proposed power grid, which is comprised of a photovoltaic system, a wind turbine, grid-supplied electricity, and a battery. This section defines the cost function of the photovoltaic system as equation (21), which is used to optimize the objective function.

$$C_{pv} = 29.55 + 1.15P_{pv} \tag{21}$$

Breakdown of Elements

1.  $C_{pv}$ :

-This represents the total cost associated with the photovoltaic system. It could encompass initial capital costs, operational and maintenance costs, or other economic factors that contribute to the overall expenditure related to the PV system.

2.  $P_{pv}$ :

-This denotes the power output of the photovoltaic system, typically measured in kilowatts (kW) or megawatts (MW). It represents the amount of electrical power generated by the solar panels at a given time.

3. Constant Term (29.55):

-This is a fixed cost component that may represent baseline expenses such as installation, fixed operational costs, or other costs that do not vary with the power output of the PV system. It indicates that there are inherent costs associated with having the system in place, regardless of how much power it generates.

4. Coefficient (1.15):

- This coefficient indicates the variable cost per unit of power generated by the PV system. In this case, it suggests that for every additional unit of power output (e.g., kW or MW), there is an additional cost of 1.15 units (e.g., dollars) associated with that power generation. This could reflect costs related to maintenance, wear and tear, or other operational expenses that increase as power production rises.

In this regard, the graphs of solar radiation and ambient temperature during 24 hours a day are shown in figures (4) and (5).

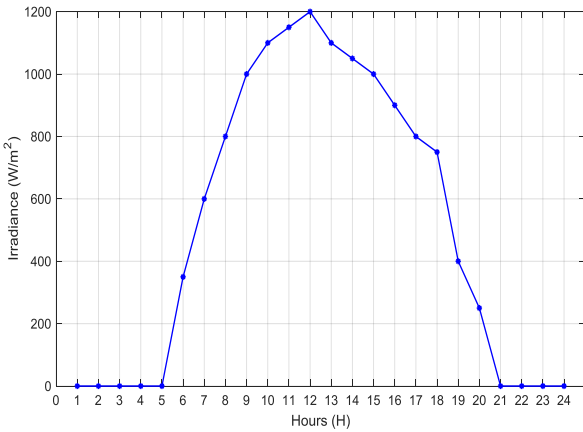


Fig. 4: Diagram of solar radiation during day and night hours

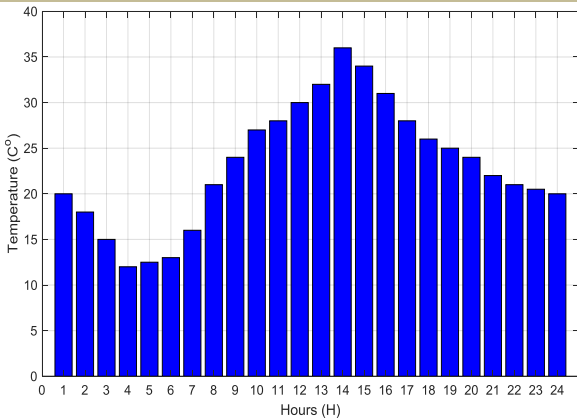


Fig. 5: Ambient temperature diagram during the day and night hours

Also, like the photovoltaic, to optimize the goal function, the price function of the WT is defined as equation (22).

$$P_{wt}(v) = \begin{cases} 0 & \text{if } v < 8 \\ P_R(0.2 + 0.02v + 0.003v^2) & \text{if } 8 < v < 12 \\ P_R & \text{if } 12 < v < 14 \\ 0 & \text{if } 4 < v \end{cases} \quad (22)$$

$$C_{wt}(P_{wt}) = 85 + 1.05P_{wt} \quad (23)$$

In this regard, the graph of wind blowing during 24 hours of the day and night is shown in figures (6).

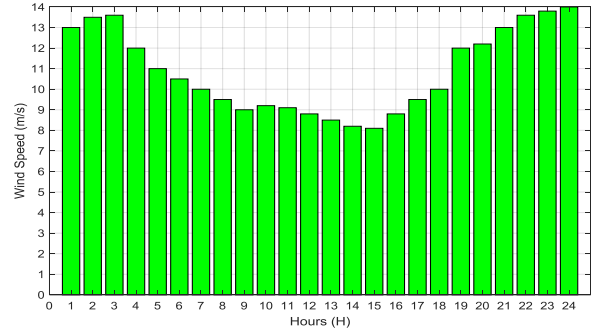


Fig. 6: Wind changes 24 hours a day

Also, the resource cost function of diesel generator and microturbine generation is defined by taking into account the emission costs to optimize the objective function, respectively (24) and (26).

$$C_{dg} = (431 + 6.53P_{dg} + 1.04 \times 10^{-4}) + CF_{Dg,t}^{EMI} \quad (24)$$

$$CF_{Dg,t}^{EMI} = (C_{CO_2} \times CO_2 + C_{SO_2} \times SO_2 + C_{NO_x} \times NO_{xDG}) \times P_{DG} \quad (25)$$

$$C_{mt} = (551.21 + 4.26P_{dg} + 0.94 \times 10^{-4}) + CF_{mt,t}^{EMI} \quad (26)$$

$$CF_{mt,t}^{EMI} = (C_{CO_2} \times CO_2 + C_{SO_2} \times SO_2 + C_{NO_x} \times NO_{xDG}) \times P_{mt} \quad (27)$$

Where  $C_{CO_2}=1.24$ ,  $C_{SO_2}=2.41$  and  $C_{NO_2}=1.28$ . Also, in this regard, the function of the emission costs of both generation sources is defined as equation (24). In this article, the electricity tariff cost function from the network is defined as equation (28), which is defined in the cost function:

$$C_{Utility} = 100 + 8.1 \times P_{utility} \quad (28)$$

In equation (24),  $C_{dg}$  is total cost associated with the diesel generator.

Constant Term (431): This represents the fixed costs, which could include installation, maintenance, and other baseline expenses that do not change with power output.

Variable Cost Term ( $6.53P_{dg}$ ): This indicates the variable cost associated with power output from the diesel generator, suggesting that for every unit increase in power generated (e.g., kW) an additional cost of 6.53 units (e.g., dollars) is incurred.

Small Constant Term ( $1.04 \times 10^{-4}$ ): This represent a negligible additional cost or correction factor that is added to the total cost.

$CF_{Dg,t}^{EMI}$ : This represents the emission cost factor associated with the diesel generator, which is calculated using equation (25).



Emission Cost Function for Diesel Generator: Equation (25),  $CF_{Dg,t}^{EMI}$ : total emission costs associated with the diesel generator.

$C_{CO_2}$ ,  $C_{SO_2}$ ,  $C_{NO_x}$ : These are the costs per unit of emissions for  $CO_2$ ,  $SO_2$ , and  $NO_x$  respectively, given as:  $C_{CO_2} = 1.24$ ,  $C_{SO_2} = 2.41$ ,  $C_{NO_x} = 1.28$ ,  $CO_2$ ,  $SO_2$ ,  $NO_x$  DG:

- These represent the quantities of  $CO_2$ ,  $SO_2$ , and  $NO_x$  emissions produced by the diesel generator.

$P_{Dg}$ : The power output from the diesel generator.

Microturbine Cost Function: Equation (26),  $C_{mt}$ : The total cost associated with microturbine generation.

Constant Term (551.21): Represents fixed costs similar to those in the diesel generator cost function.

- Variable Cost Term ( $4.26 P_{mt}$ ): Indicates the variable cost associated with power output from the microturbine.

- Small Constant Term ( $0.94 \times 10^{-4}$ ): A negligible additional cost or correction factor.

-  $CF_{mt,t}^{EMI}$ :

- Emission cost factor associated with the microturbine, calculated using equation (27).

Emission Cost Function for Microturbine:

-Equation (27)

$$CF_{mt,t}^{EMI} = (C_{CO_2} \times Co_2 + C_{SO_2} \times So_2 + C_{NO_x} \times NO_{x\_mt}) \times P_{mt}$$

- Similar structure to equation (25), but applies to emissions from microturbines.

Utility Electricity Tariff Cost Function:

Equation (28)

-  $C_{Utility}$ :

- Total cost of purchasing electricity from the utility grid.

- Constant Term (100):

- Represents fixed costs associated with accessing utility electricity such as connection fees or base charges.

- Variable Cost Term ( $8.1 P_{utility}$ ):

- Indicates the variable cost associated with the amount of electricity consumed from the utility, suggesting a cost of 8.1 units (e.g., dollars) per unit of power consumed.

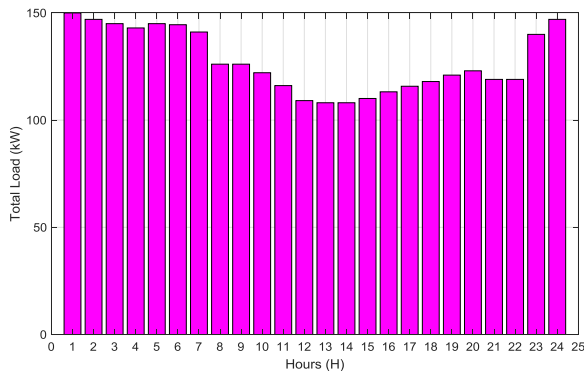


Fig. 7: Graph of total loads per hour

### 3.2. Results and Discussion

The multi-objective particle algorithm is used to optimize the goal function defined by equation (20) of the third part as illustrated in figure (8).

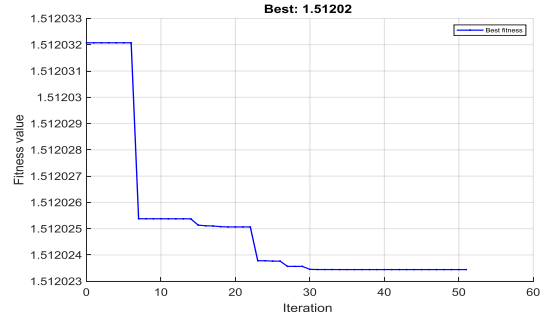


Fig. 8: The optimization process of the objective function using the multi-objective particle algorithm

The results of optimization for the power generation of different sources are shown in figure (9).

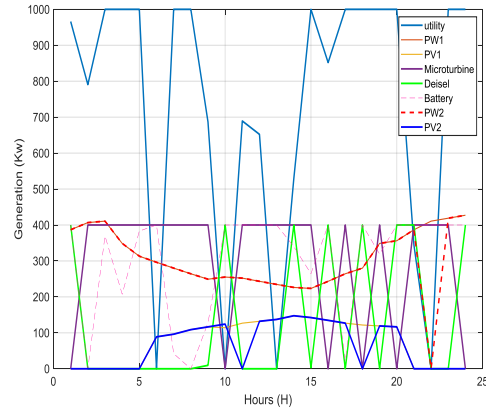


Fig. 9: The results of optimization for power generation in different sources in two dimensions

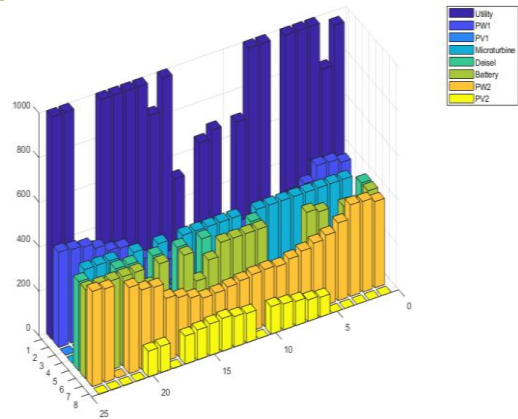


Fig. 10: The results of optimal power generation of different sources in 24 hours a day in three dimensions

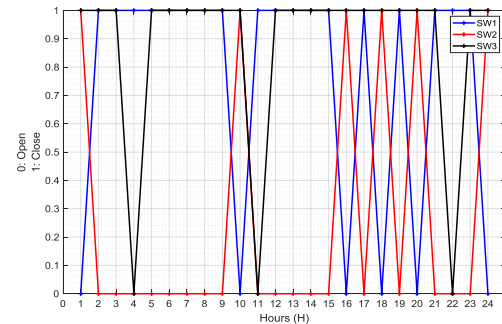
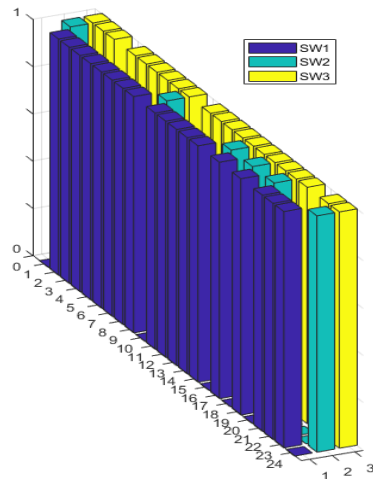
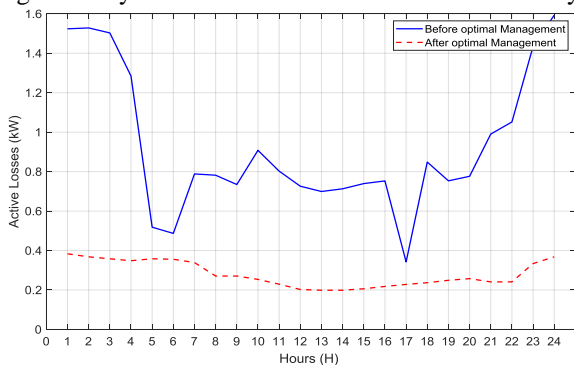


Fig. 11: The results of optimizing the connection and non-connection of microgrids to the main distribution network in 24 hours of a day (two-dimensional format)



**Fig. 12:** The results of optimizing the connection and non-connection of microgrids to the main distribution network in 24 hours of a day (Three-dimensional format)

Diagrams (13) through (15) display the network voltage deviation and active and reactive loss curves at various hours, respectively. As it can be seen in these figures, the network's active and reactive losses have dramatically dropped throughout all hours following the resources' optimal output power distribution, and the amount of voltage deviation has also improved significantly in all hours and has decreased favourably.



**Fig. 13:** The amount of network active losses during 24 hours before and after optimal energy management

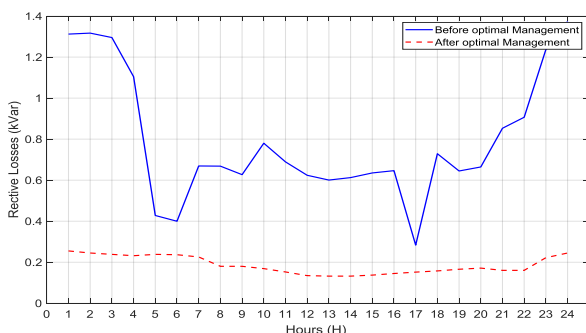


**Fig. 14:** The amount of network reactive losses during 24 hours before and after optimal energy management

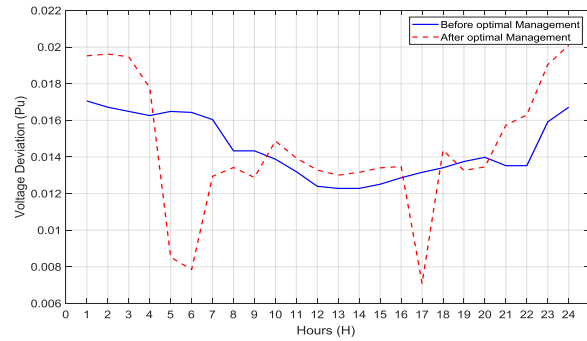


**Fig. 15.** The amount of network voltage deviation during 24 hours before and after optimal energy management

## 4. Conclusion

The best way to manage power in the distribution networks, made up of several microgrids in various connected and disconnected states, was examined in this article. The research uses a hierarchical design methodology. An economic modeling of all distributed generation systems was carried out, and the operating costs of the energy system within the network, by utilizing the particle algorithm, were minimized by considering factors such as losses and voltage deviation.

The article focused on the investigation and simulation of the proposed energy management program in the 33-bus distribution network that included three microgrids with diverse distributed generation sources. A novel multi-objective approach was employed. The study encompassed the examination of technical and economic aspects of electricity distribution within both independent and grid-connected microgrids, incorporating hybrid power generation sources and energy storage units. The analysis took into account various values such as capital price, operating price, fuel price, energy price, emission fines, and general costs. Simulation results demonstrated the effectiveness of the proposed method in optimizing the operating costs of the distribution network and microgrids. Additionally, the method considered the optimal integration and disintegration of microgrids throughout a 24-hour period, utilizing a hierarchical control plan.

## References

- [1] Guo, Y., Lin, Y., Sun, M., "The impact of integrating distributed generations on the losses in the smart grid", IEEE Power and Energy Society General Meeting, pp. 1-6, 2011, <https://doi.org/10.1002/er.6984>.
- [2] Jauch, E. T., "Possible effects of smart grid functions on LTC transformers", IEEE Transactions on Industry Applications, Vol. 47, No. 2, pp. 1013-1021, 2010, <https://doi.org/10.1109/TIA.2010.2101993>.

- [3] Chen, C., Duan, S., Cai, T., Liu, B., Hu, G., "Smart energy management system for optimal microgrid economic operation", IET renewable power generation, Vol. 5, No. 3, pp. 258-267, 2011, <https://doi.org/10.1049/iet-rpg.2010.0052>.
- [4] Niknam, T., Abarghoee, R. A., Narimani, M. R., "An efficient scenario-based stochastic programming framework for multi-objective optimal micro-grid operation", Applied Energy, Vol. 99, pp. 455-470, 2012, <https://doi.org/10.1016/j.apenergy.2012.04.017>.
- [5] Chakraborty, S., Weiss, M. D., Simoes, M. G., "Distributed intelligent energy management system for a single-phase high-frequency AC microgrid", IEEE Transactions on Industrial electronics, Vol. 54, No. 1, pp. 97-109, 2007, <https://doi.org/10.1109/TIE.2006.888766>.
- [6] Marnay, C., Venkataramanan, G., Stadler, M., Siddiqui, A. S., Firestone, R., Chandran, B., "Optimal technology selection and operation of commercial-building microgrids", IEEE Transactions on Power Systems, Vol. 23, No. 3, pp. 975-982, 2008, <https://doi.org/10.1109/TPWRS.2008.922654>.
- [7] De Souza, B. A., De Almeida, A. M. F., "Multi objective optimization and fuzzy logic applied to planning of the volt/var problem in distributions systems", IEEE Transactions on Power Systems, Vol. 25, No. 3, pp. 1274-1281, 2010, <https://doi.org/10.1109/TPWRS.2010.2042734>.
- [8] Niknam, T., Zare, M., Aghaei, J., "Scenario-based multi objective volt/var control in distribution networks including renewable energy sources", IEEE Transactions on Power Delivery, Vol. 27, No. 4, pp. 2004-2019, <https://doi.org/10.1109/TPWRD.2012.2209900>.
- [9] Zhu, J. Z., "Optimal reconfiguration of electrical distribution network using the refined genetic algorithm", Electric Power Systems Research, 2002, Vol. 62, No. 1, pp. 37-42, 2012, [https://doi.org/10.1016/S0378-7796\(02\)00041-X](https://doi.org/10.1016/S0378-7796(02)00041-X).
- [10] Paudyal, S., Canizares, C. A., Bhattacharya, K., "Optimal operation of distribution feeders in smart grids", IEEE Transactions on Industrial Electronics, Vol. 58, No. 10, pp. 4495-4503, 2011, <https://doi.org/10.1109/TIE.2011.2112314>.
- [11] De Paepe, M., Herdt, P. D., Mertens, D., "Micro-CHP systems for residential applications", Energy conversion and management, Vol. 47, No. 18-19, pp. 3435-3446, 2006, <https://doi.org/10.1016/j.enconman.2005.12.024>.
- [12] Ren, H., Gao, W., "Economic and environmental evaluation of micro CHP systems with different operating modes for residential buildings in Japan", Energy and Buildings, Vol. 42, No. 6, pp. 853-861, 2010, <https://doi.org/10.1016/j.enbuild.2009.12.007>.
- [13] Robert Zogg, P., Brodrick, J., "Using CHP systems in commercial buildings", Ashrae Journal, Vol. 47, No. 9, 2005, <https://citeseerx.ist.psu.edu/document?repid=rep1&type=pdf&doi=6b7a4c5d0c41dc059c67d3a89ab2ca012c1f62c>.
- [14] Lorestani, A., Ardehali, M., "Optimization of autonomous combined heat and power system including PVT, WT, storages, and electric heat utilizing novel evolutionary particle swarm optimization algorithm", Renewable Energy, Vol. 119, pp. 490-503, 2018, <https://doi.org/10.1016/j.renene.2017.12.037>.
- [15] Bornapour, M., Hooshmand, R. A., Khodabakhshian, A., and Parastegari, M., "Optimal stochastic scheduling of CHP-PEMFC, WT, PV units and hydrogen storage in reconfigurable micro grids considering reliability enhancement", Energy Conversion and Management, Vol. 150, pp. 725-741, 2017, <https://doi.org/10.1016/j.enconman.2017.08.041>.
- [16] Bornapour, M., Hooshmand, R. A., Parastegari, M., "An efficient scenario-based stochastic programming method for optimal scheduling of CHP-PEMFC, WT, PV and hydrogen storage units in micro grids", Renewable energy, Vol. 130, pp. 1049-1066, 2019, <https://doi.org/10.1016/j.renene.2018.06.113>.
- [17] Maleki, A., Hafeznia, H., Rosen, M. A., Pourfayaz, F., "Optimization of a grid-connected hybrid solar-wind-hydrogen CHP system for residential applications by efficient metaheuristic approaches", Applied Thermal Engineering, Vol. 123, pp. 1263-1277, 2017, <https://doi.org/10.1016/j.applthermaleng.2017.05.10>.
- [18] Aluisio, B., Dicatorato, M., Forte, G., Trovato, M., "An optimization procedure for Microgrid day-ahead operation in the presence of CHP facilities", Sustainable Energy, Grids and Networks, Vol. 11, pp. 34-45, 2017, <https://doi.org/10.1016/j.segan.2017.07.003>.
- [19] Guangqian, D., Bekhrad, K., Azarikhah, P., Maleki, A., "A hybrid algorithm based optimization on modeling of grid independent biodiesel-based hybrid solar/wind systems" Renewable Energy, Vol. 122, pp. 551-560, 2018, <https://doi.org/10.1016/j.renene.2018.02.021>.
- [20] Fardini, A., Ahmadian, A., Golkar, M. A., "Optimal energy management of a distribution network connected to different microgrids based on game theory approach", Iranian Electric Industry Journal of Quality and Productivity, Vol. 7, No. 2, pp. 30-46, 2019, <http://iejqp.ir/article-1-522-en.html>.
- [21] Terzija, V. V., "Adaptive under frequency load shedding based on the magnitude of the disturbance estimation", IEEE Trans. on Power Systems, Vol. 21, No. 3, August, 2006, <https://doi.org/10.1109/TPWRS.2006.879315>.
- [22] Farahani, B., Abedi, M., "An optimal load-shedding scheme during contingency situations using meta-heuristics algorithms with application of AHP method", 11th International on Optimization of Electrical and Electronic Equipment, pp. 167-173, 22-24, May 2008, <https://doi.org/10.1109/OPTIM.2008.4602361>.
- [23] Kundur, P., "Power System Stability and control", McGrawHill, USA 1994, <https://taylorfrancis.com/chapters/edit/10.4324/b12113-10/power-system-stability-prabha-kundur>.
- [24] Jin, J., Liu, Y., Li, P., Chang, M., "Cooperative resilience of cyber-physical power systems under hybrid attacks via dynamic topology", Frontiers in Energy Research, 10, 887870, 2022, <https://doi.org/10.3389/fenrg.2022.887870>.
- [25] Chung, H. M., Li, W. T., Yuen, C., Chung, W. H., Zhang, Y., Wen, C. K., "Local cyber-physical attack for masking line outage and topology attack in smart grid", IEEE Transactions on Smart Grid, 10(4), 4577-4588, 2018, <https://doi.org/10.1109/TSG.2018.2865316>.
- [26] Acosta, M. R. C., Ahmed, S., Garcia, C. E., Koo, I., "Extremely randomized trees-based scheme for stealthy cyber-attack detection in smart grid networks", IEEE access, 8, 19921-19933, 2020, <https://doi.org/10.1109/ACCESS.2020.2968934>.

- [27] Khademi, M. M., Kazemi, E., Jahromi, M. Z., "*Optimal probability placement of the charge station of electric vehicles in a distributed power network containing the dg using the queuing theory*", In 2023 31st International Conference on Electrical Engineering ICEE, pp. 133-143, May 2023, <https://doi.org/10.1109/ICEE59167.2023.10334824>.
- [28] Al-Zaidi, W. K. M., Inan, A., "*Optimal placement of battery swapping stations for power quality improvement: a novel multi techno-economic objective function approach*", Energies, 17(1), 110, 2023, <https://doi.org/10.3390/en17010110>.